Preliminary results from a multiscale approach to modeling plasma surface interactions involving tungsten

Davide Curreli* on behalf of Brian D. Wirth+,#, and

Institution	Principal Investigator	Additional Personnel
ANL	Barry Smith (FASTMath)	Danqing Wu (FASTMath)
GA/DIII-D	Phil Snyder	Rui Ding, Adam McLean (LLNL), Vincent Chan
LANL	Xianzhu Tang	Jim Ahrens & Li-Ta "Ollie" Lo (SDAV), Sham Bhat & David Higdon (QUEST), Danny Perez, Luis Sandoval, Art Voter, Blas Uberuaga
ORNL*	**Brian Wirth***	Alexander Barashev, **David Bernholdt****, Ozgur Cekmer, Sophie Blondel, John Canik, Ane Lasa, Jeremy Meredith (SDAV), Phil Roth (SUPER), German Samolyuk, Roger Stoller
PNNL	Rick Kurtz	Giridhar Nandipati, Ken Roche, Wahyu Setyawan
UCSD	Serge Krasheninnikov	Jerome Guterl, Roman Smirnov
UIUC	David Ruzic and Davide Curreli	Kishor Kalathiparambil, Jon Drobny, Ivan Shchelkanov
UMass-Amherst	Dimitrios Maroudas	Lin Hu
U Missouri	Karl Hammond	
UTK	Brian Wirth	Mary Alice Cusentino, Donghua Xu, Eric Yang, Tim Younkin

In partnership with:

Project web site:
https://collab.mcs.anl.gov/display/PSIscidac/

* dcurreli@illinois.edu
+ bdwirth@utk.edu

Presented at the IAEA CRP Meeting September 2015

#

This work was supported by the U.S. Department of Energy, Office of Fusion Energy Sciences and and Advanced Scientific Computing Research (ASCR) through the SciDAC-3 program.

The Challenge: No current materials are viable to bridge the significant gap between today's tokamaks & future fusion reactors

C-Mod Molybdenum (T_{melt}=2900 K) limiter melted during disruptions

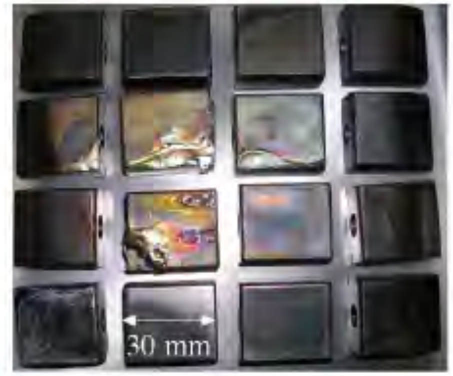

Issue / Parameter	Present Tokamaks	ITER	DEMO	Consequences
Quiescent energy exhaust *GJ / day*	~ 10	3,000	60,000	- active cooling - max. tile thickness ~ 10 mm
Transient energy exhaust from plasma instabilities *$\Delta T \sim MJ / A_{wall}(m^2) / (1\ ms)^{1/2}$*	~ 2	15	60	- require high $T_{melt/ablate}$ - limit? ~ 60 for C and W - surface distortion
Yearly neutron damage in plasma-facing materials *displacements per atom*	~ 0	~ 0.5	20	- evolving material properties: thermal conductivity & swelling
Max. gross material removal rate with 1% erosion yield *(mm / operational-year)*	< 1	300	3000	- must redeposit locally - limits lifetime - produces films
Tritium consumption *(g / day)*	< 0.02	20	1000	- Tritium retention in materials and recovery

- Dilute MFE plasma ($n \sim 10^{20}\ m^{-3}$) extinguished by small particulate
  - 2 mm "drop" of W == $N_{e,ITER}$

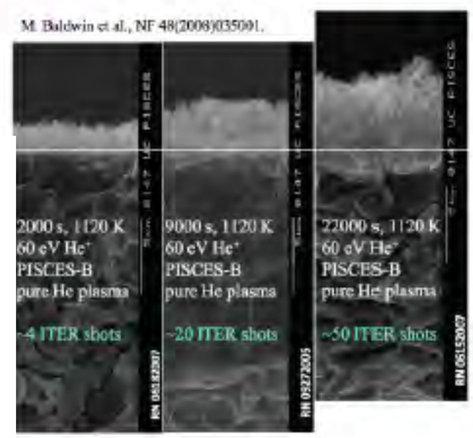

ITER's current operating plans involve a tungsten divertor with initial He plasma operation: significant concern about sub-surface helium bubble formation & surface morphology changes influencingcore plasma performance, tritium retention, and/or tritium-containing dust

PSI Perspective & Objective

- Objective is to develop PSI simulation capability across three coupled spatial regions:
  - **Edge/scrape-off-layer region of the plasma, with sheath effects**
  - **Near surface material response to plasma exhaust, with neutron damage and influenced/coupled to plasma sheath**
  - **Structural materials response to intense, 14 MeV-peaked neutron spectrum**

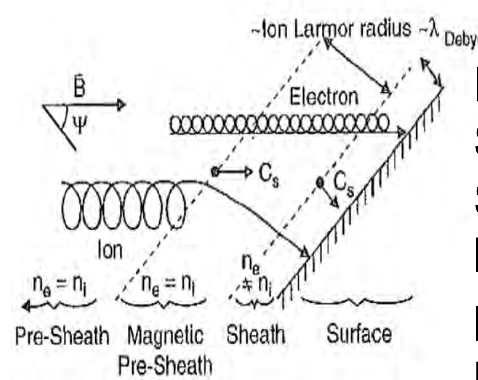

Plasma Edge Scrape Off Layer Sheath – heat & particle flux, recycling, etc.

mm

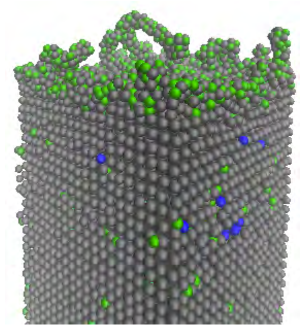

Material surface - erosion (impurity & dust), T retention, surface evolution

10^2 – 10^3 nm

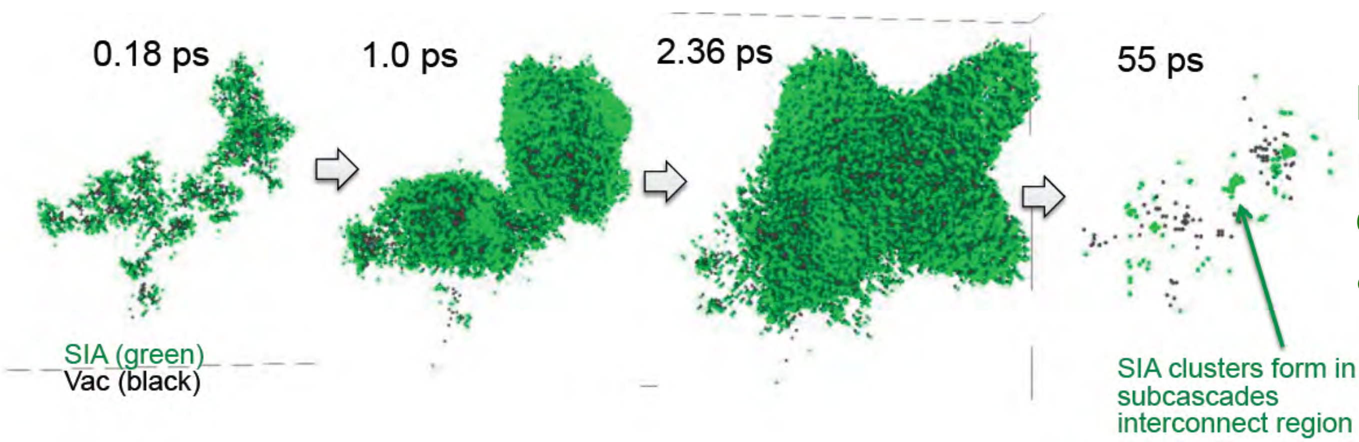

Material bulk – neutron damage & transmutation

10^{-3} – 10^2 mm

*Multiscale modeling capability – a work in progress**

Goal: Discovery science to identify Mechanisms of W nano-scale fuzz formation and synergies between He & H exposure that impact D/T permeation & retention – and surface mass loss (dust)

Mechanisms of interest: sputtering, surface adatom formation, diffusion, He bubble formation, expansion & rupture

Focus on MD & kinetic modeling approaches, leading to a large-scale continuum-level reaction-diffusion code for plasma materials interactions & Developing the connections across the interface

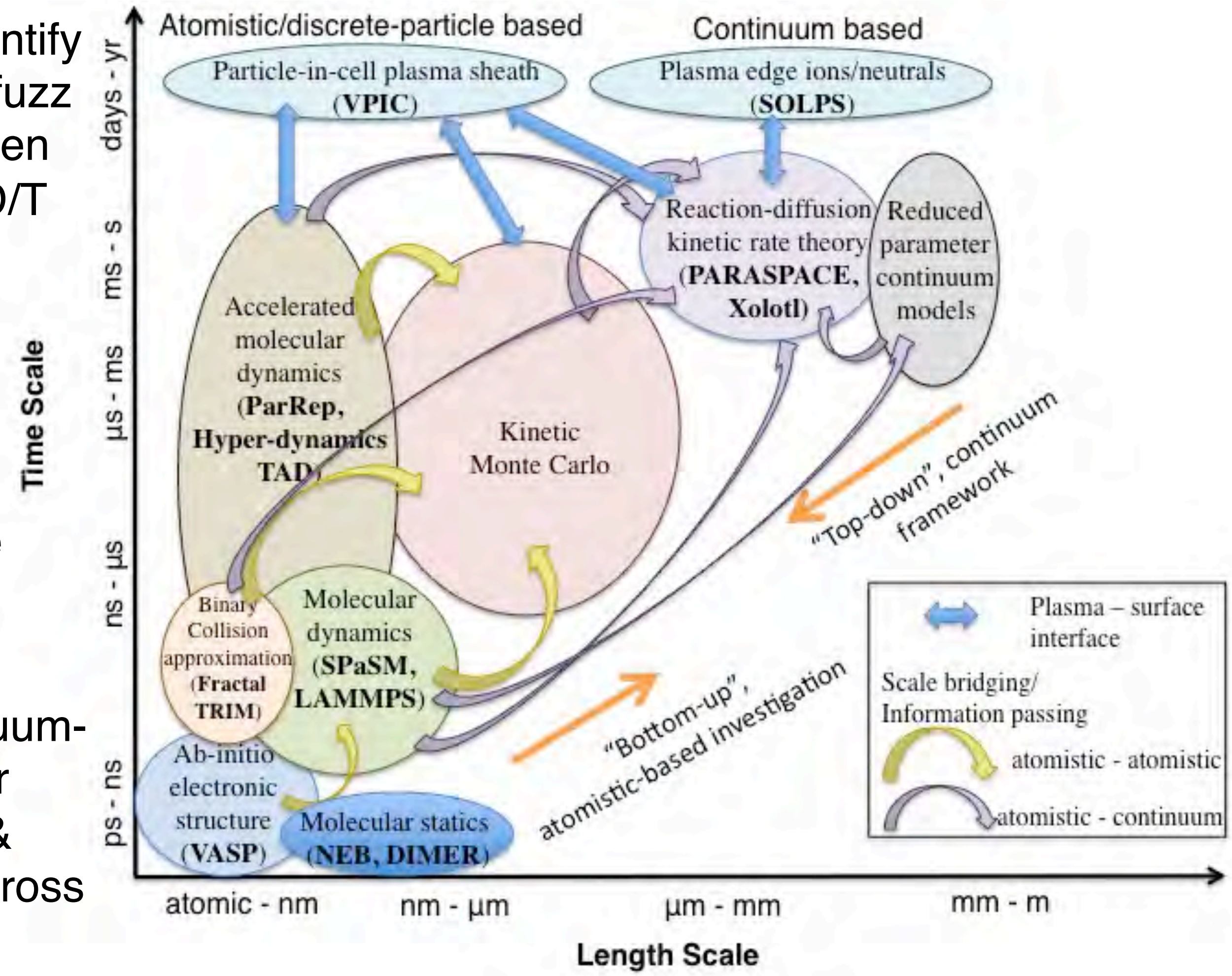

Biggest long-term scientific challenge is understanding the kinetics of coupled defect – impurity evolution with a disparate range of kinetic rates --- this requires algorithmic improvements on both the physics and computing side

* BD Wirth, K.D. Hammond, S.I. Krashenninikov, and D. Maroudas, "Challenges and Opportunities of Modeling Plasma Surface Interactions in Tungsten using High Performance Computing, *Journal of Nuclear Materials* ***463*** (2015) 30-38.

Impurity transport code (ERO) modeling of refractory metal erosion in DIII-D DiMES probe

The ERO code:

- Plasma-surface interaction
- Local impurity transport

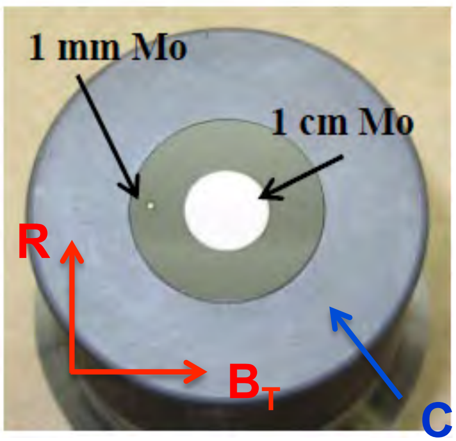

- Thin Mo/W film on Si substrate.
- Erosion & deposition determined by Rutherford backscattering (RBS) measurements.
- 1 cm sample for net erosion and 1 mm sample for gross erosion.
- L-mode deuterium discharges, lower single null configuration.

- **New geometry implemented into ERO**
- **OEDGE backgroud plasma as input: n_e, T_e, $E_{//}$**
- **Magnetic field: B_t = 2.25 T pitch angle:1.5°**
- **Impurities: C^{3+}**
- **Chemical erosion yield: Roth formula**
- **Homogeneous material mixing model**

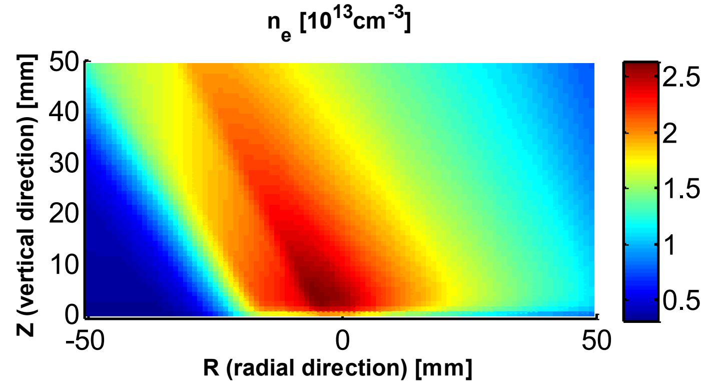

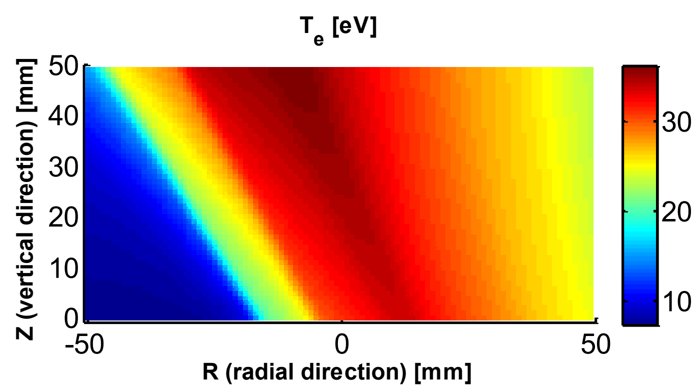

Predicted erosion agrees well with experiment

C concentration in background plasma 1.8%

	Mo		W	
	EXP	ERO	EXP	ERO
Net erosion rate (nm/s)	0.42	0.43	0.18	0.14
Redeposition ratio (1cm)	44 % (46%)	39 %	63% (67%)	67%
Redeposition ratio (1mm)	N/A	4 %	N/A	14%

- **W re-deposition ratio is much higher due to its shorter ionization length (~1 mm)**

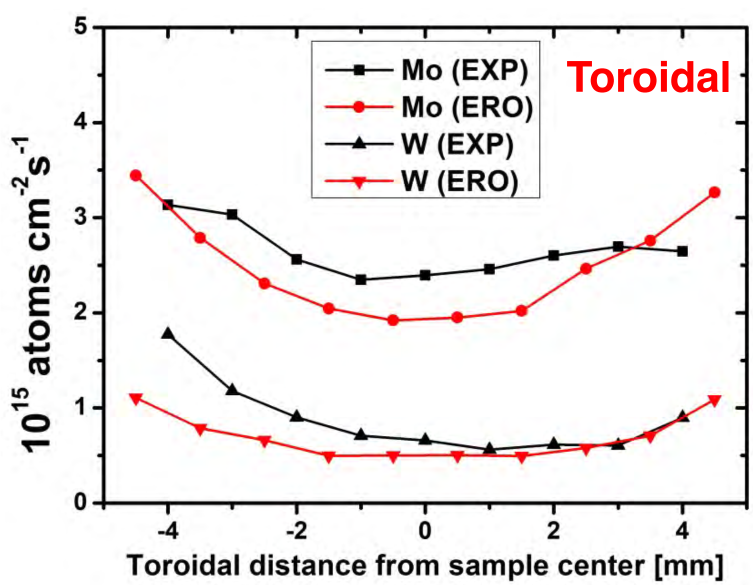

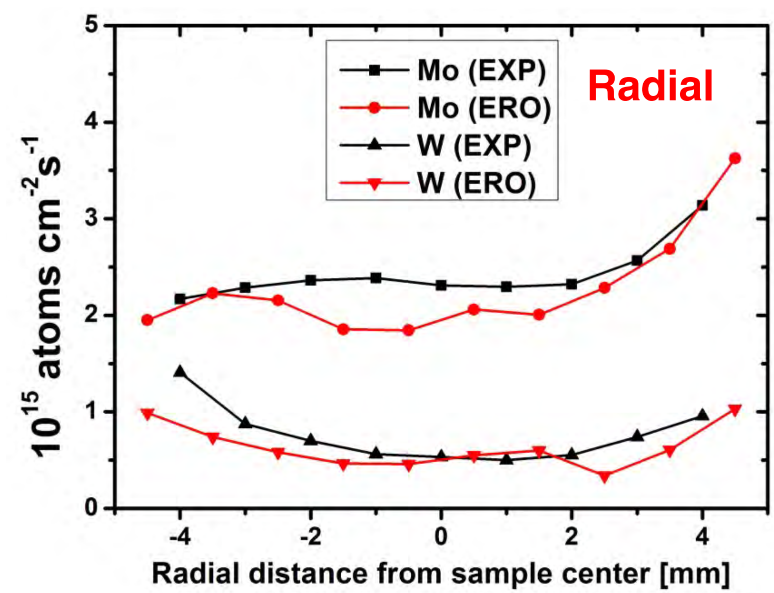

R. Ding, V. Chan (GA-DIII-D), manuscript in preparation

Plasma Sheath Effects using a Particle-in-Cell model

Ion Energy-Angle Distribution in Magnetized Plasma Sheath

- Plasma Sheath: establishes the link between “Edge” and “Wall”
- When the plasma is approaching a material wall, finite-gyro-orbit effects are not negligible, and the typical gyro-center and drift-kinetics approximations are no longer valid.
- UIUC full-f 6D sheath PIC code used to analyze the near-wall ion kinetics
- PIC Characterization of the Ion Energy-Angle Distributions (IEAD) in oblique magnetic fields
- IEAD are a necessary input to material & PMI models

Ion Energy-Angle Distribution functions at the Wall from PIC

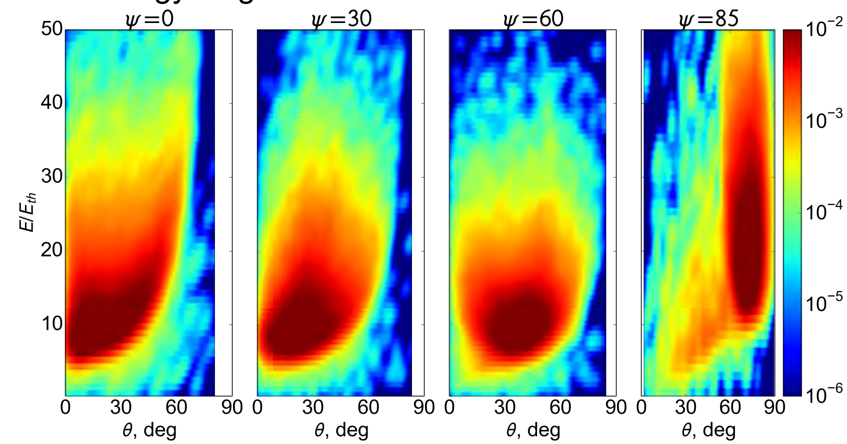

Ion Angular Distribution at the Wall from PIC

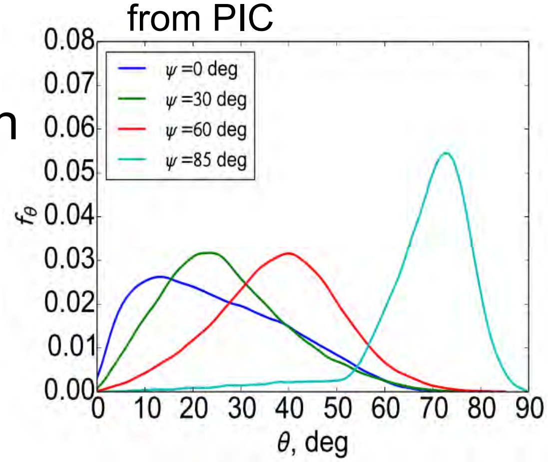

Trend of the average ion impact angle at the wall, and comparison with other results from literature

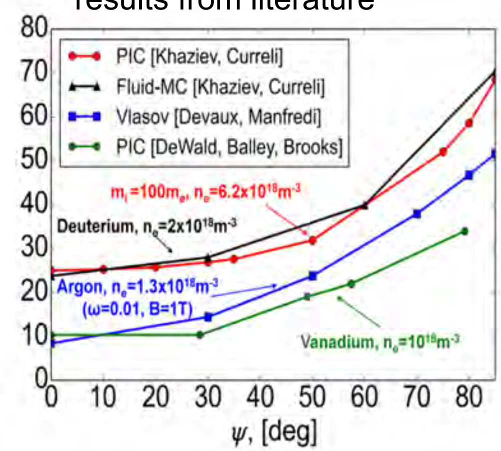

R. Khaziev, D. Curreli, "Ion energy-angle distribution functions at the plasma-material interface in oblique magnetic fields", *Phys. Plasmas* **22** (2015) 043503.

Initial modeling of surface evolution on sputtering

Development of advanced binary collision approximation models (Fractal-TRIDYN) including surface roughness and dynamic composition

- Finite surface roughness and surface morphology affect the sputtering processes and the impurity release
- Improved Fractal-TRIDYN algorithm decreases computational complexity from $O(n^2)$ to $O(n)$, with x20 gain in computational speed
- In addition, a new approach based on a statistical description of surface morphology has been developed
- New statistical algorithm reproduces same results of Fractal-TRIDYN
- Statistical algorithm is x28 faster than the improved O(n) fractal algorithm

Typical run (10k particles, 300 eV, He on Be):

TRIDYN:	D=2.000, 1900KB, 9.7 sec
FTRIDYN:	D=2.075, 2700 KB, 543 sec
Statistical FTRIDYN:	3200A, 2700 KB, 19 sec

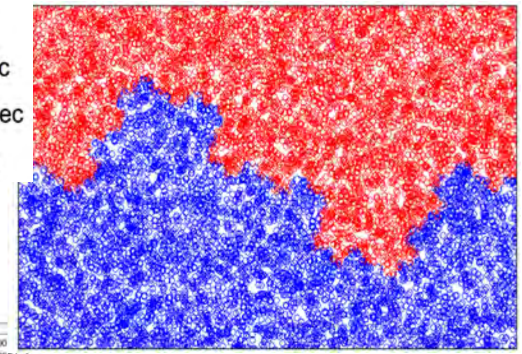

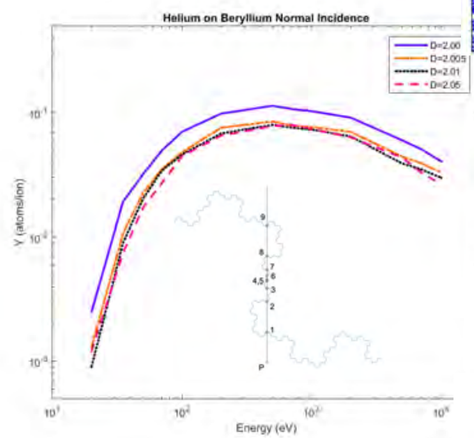

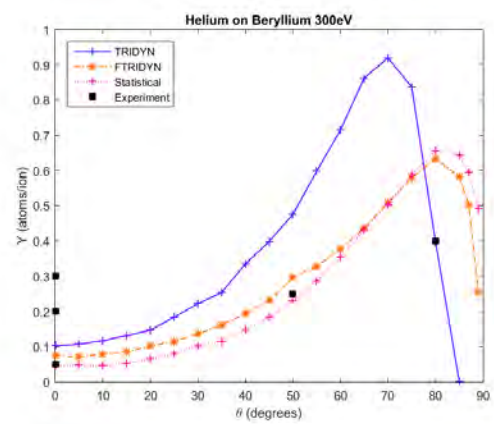

J. Drobny, D. Curreli and D. Ruzic (UIUC), manuscripts in preparation

Key MD observations of early stage He bubble evolution

- **Helium insoluble but highly mobile and can self-trap (at high implantation rates) due to strong He-W repulsion to form highly mobile, strongly bound helium clusters – *implantation rate effects are very important***

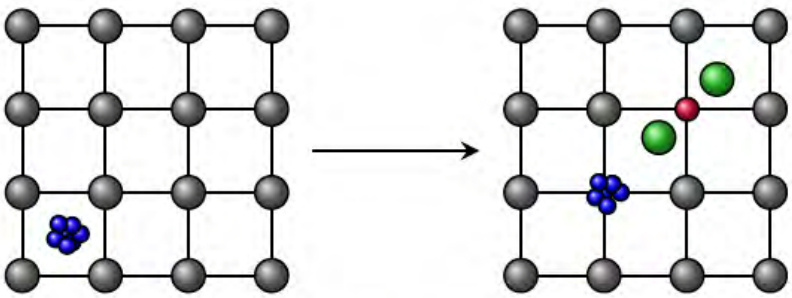

"trap mutation" processes

Occurs when 6–9 helium atoms coalesce, depending on temperature, after which bubble grows by absorbing smaller clusters.

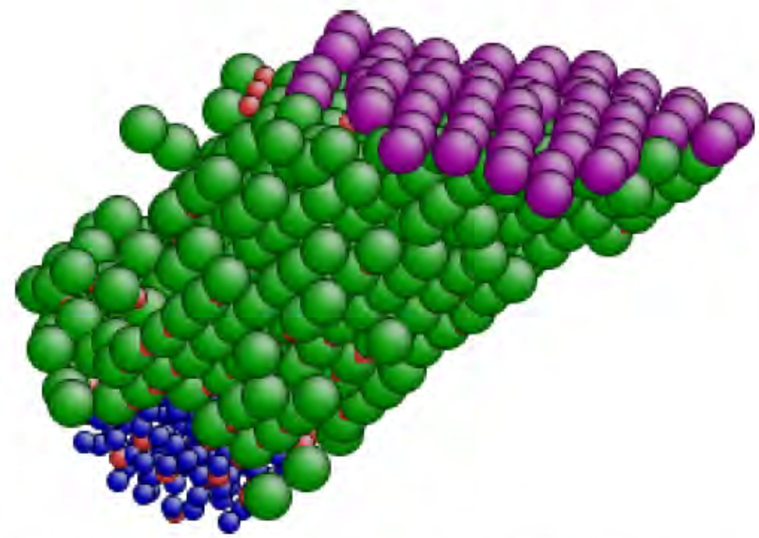

"loop-punching" processes

Movie available with F. Sefta, *et al. Nucl. Fusion* **53**: 073015 (2013)

- **Significant surface evolution through tungsten adatom formation, driven by trap mutation and loop-punching as tungsten interstitials rapidly diffuse to surface**
- ***As bubbles continue to grow at very high pressure, eventually rupture***

A brief word about Molecular Dynamics (MD) calculations

- "Common" MD codes: LAMMPS, SPASM
- Typically run on small clusters (usually because of throughput), especially for 'discovery' science
- Increasingly used for 10^7 atoms & beyond (provide decreased implantation rates)
- Limited by interatomic potentials and achievable timescales

Bursting of He bubble onto W surface

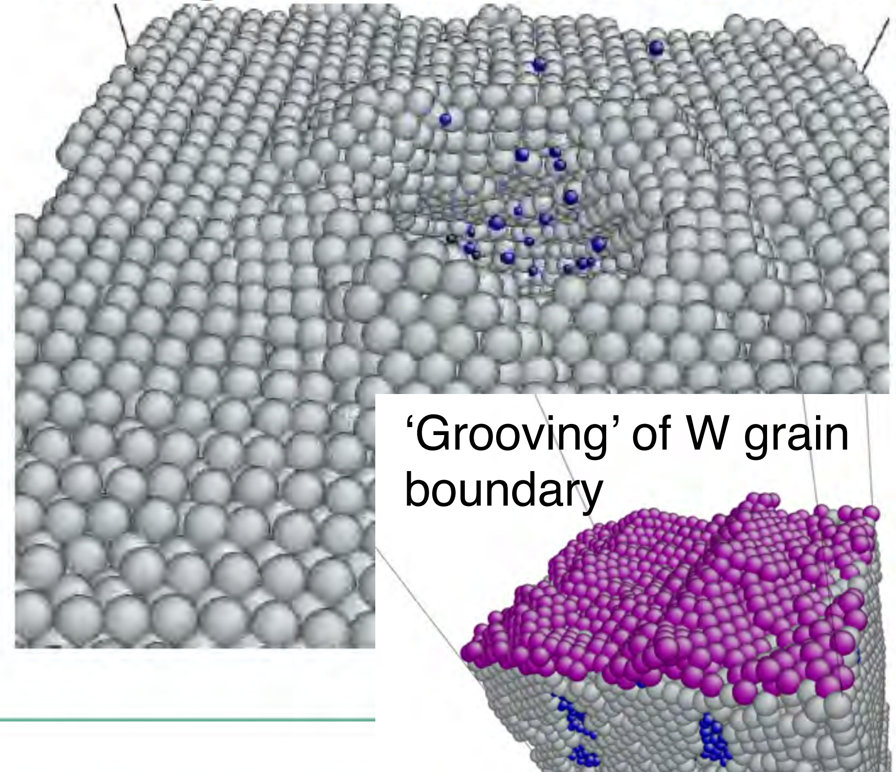

'Grooving' of W grain boundary

The Time Scale Challenge

- 1 MD time step, $O(10^{-15}$ s) requires 1 ms (10^{-3} s) wallclock time
  - Typical for $O(2\text{x}10^7$ atoms), $O(2\text{x}10^4$ cores) on Mira (ANL)
- Simulating onset of fuzz formation (10^4 s) requires **O(300 M years)**
  - Completely unrealistic extrapolation to exascale: "only" **O(80k years)**

Tungsten surface response to low-energy He exposure

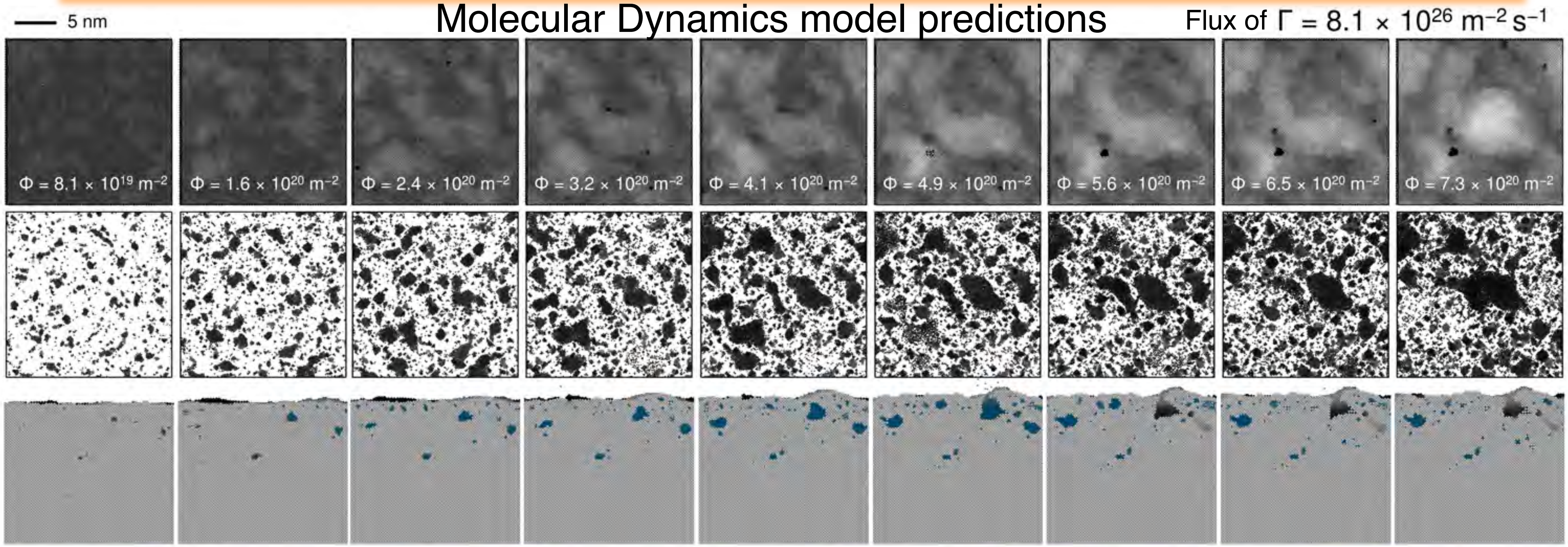

High-flux simulations showing surface growth and helium accumulation below a W(100) surface. Top: View of surface (white = +1.5 nm, black = –2 nm); Middle: helium atoms, top view (black = at surface, white = –15 nm); Bottom: cross-section.

- MD* of 100 eV He implanted into W reveals formation and growth of over-pressurized, sub-surface He bubbles thru self-trapping, trap mutation, loop punching and bubble bursting that evolve tungsten surface (hillocks & craters)

  → Qualitatively consistent with experiments** of W surface evolution following 60 eV He on tungsten

  → Quantitative comparison requires evaluation of rate & scale effects (Γ:MD 10^{26} vs expt 10^{19}; Φ: 10^{20} vs 10^{24})

Experiment: $\Gamma = 3\text{x}10^{19}$ m^{-2}s^{-1}
$\Phi = 3\text{x}10^{24}$ m^{-2}

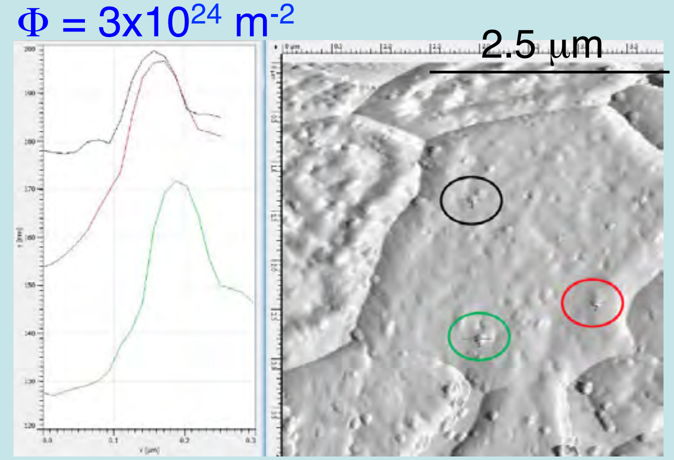

* Hammond & Wirth, UTK/ORNL

** Donovan, Buchenauer, Kolasinksi et al., SNL

Accelerated MD simulations of rate effects on near-surface helium bubbles with rates approaching ITER relevance

First simulation of He bubble growth at He-irradiation flux appropriate for fusion first-wall in ITER. The simulations find a qualitatively different growth mode when rates approach experimental values. They reveal rate effects on bubble size, shape, pressure, and surface damage.

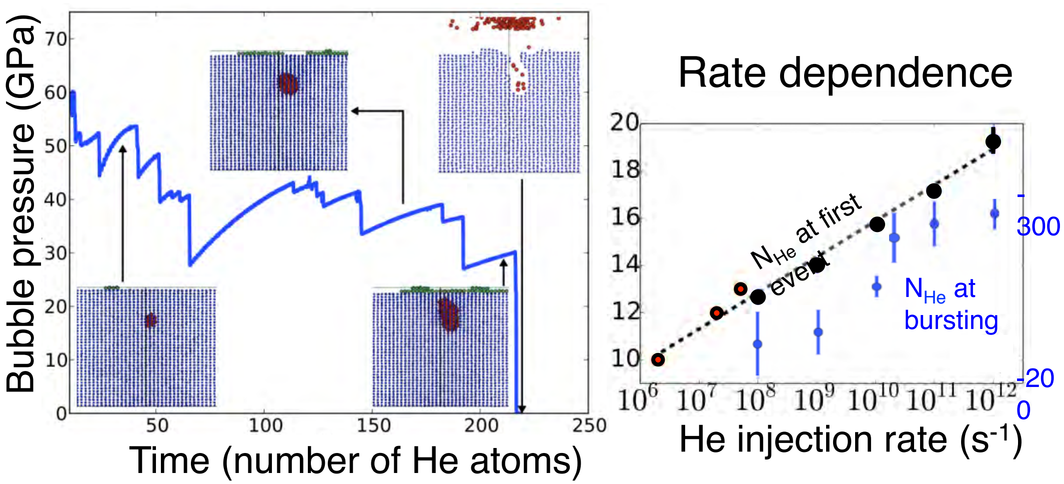

Left: Growth/bursting at intermediate (near-crossover) rate (10^9 He/s). Helium pressure is relieved via emission of W interstitials. At slower growth rates, interstitials have time to diffuse over surface of bubble, ultimately emitting more interstitials from top in the form of dislocation loops (crowdion clusters) that travel to surface, leaving adatoms. Right: Dependence of bubble properties on bubble growth rate.

Research

Parallel Replica Dynamics simulations of bubble growth with He injection rate ranging from 10^{12} s^{-1} to $2x10^6$ s^{-1}. Efficient to petascale: utilized 160,000 cores (over half of Titan) at ORNL at 77% efficiency.

Slower growth leads to smaller, more anistropic bubble that grows in a directed way towards surface, producing fewer adatoms during growth and creating less surface damage upon bursting.

Collaboration with BES program Accelerated Molecular Dynamics (Voter) at LANL.

L. Sandoval, D. Perez, B.P. Uberuaga, and A.F. Voter; *Physical Review Letters* **114** (2015) 105502 (2015). Work performed at LANL, computing at ORNL. **OLCF and DOE Office of Science highlight**

*Impact of surface orientation**

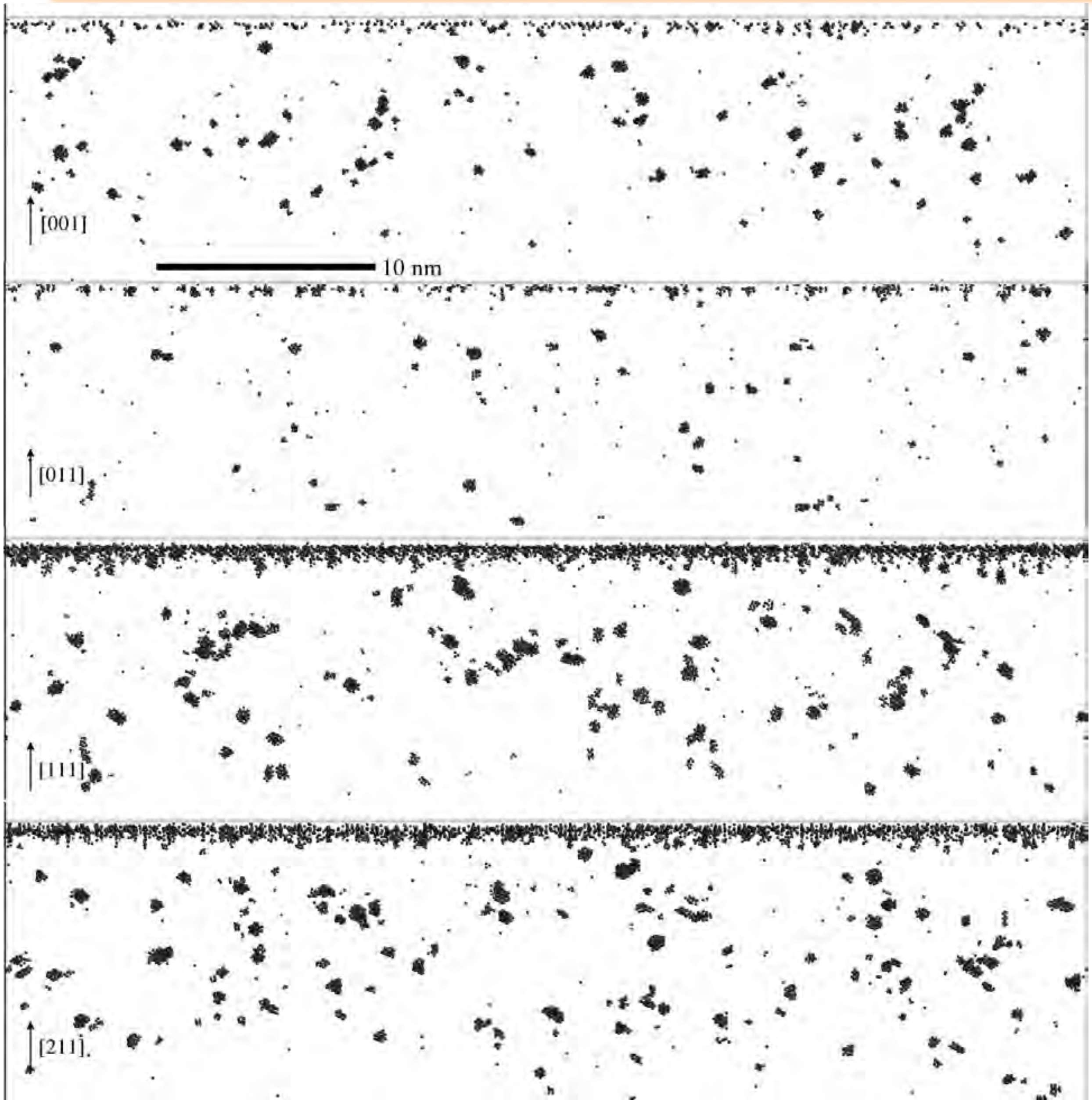

Helium distributions at a fluence of 10^{19} He-m^{-2}

Nominal Flux:
4.0×10^{25} He-m^{-2} s^{-1} of 100 eV He (thermally implanted)
Temperature: 933K

Note presence of concentrated He layer in (111) and (211) cases – surface orientation strongly influences helium retention

* Hammond and Wirth, *JAP* **116** (2014) 143301

*Impact of surface orientation**

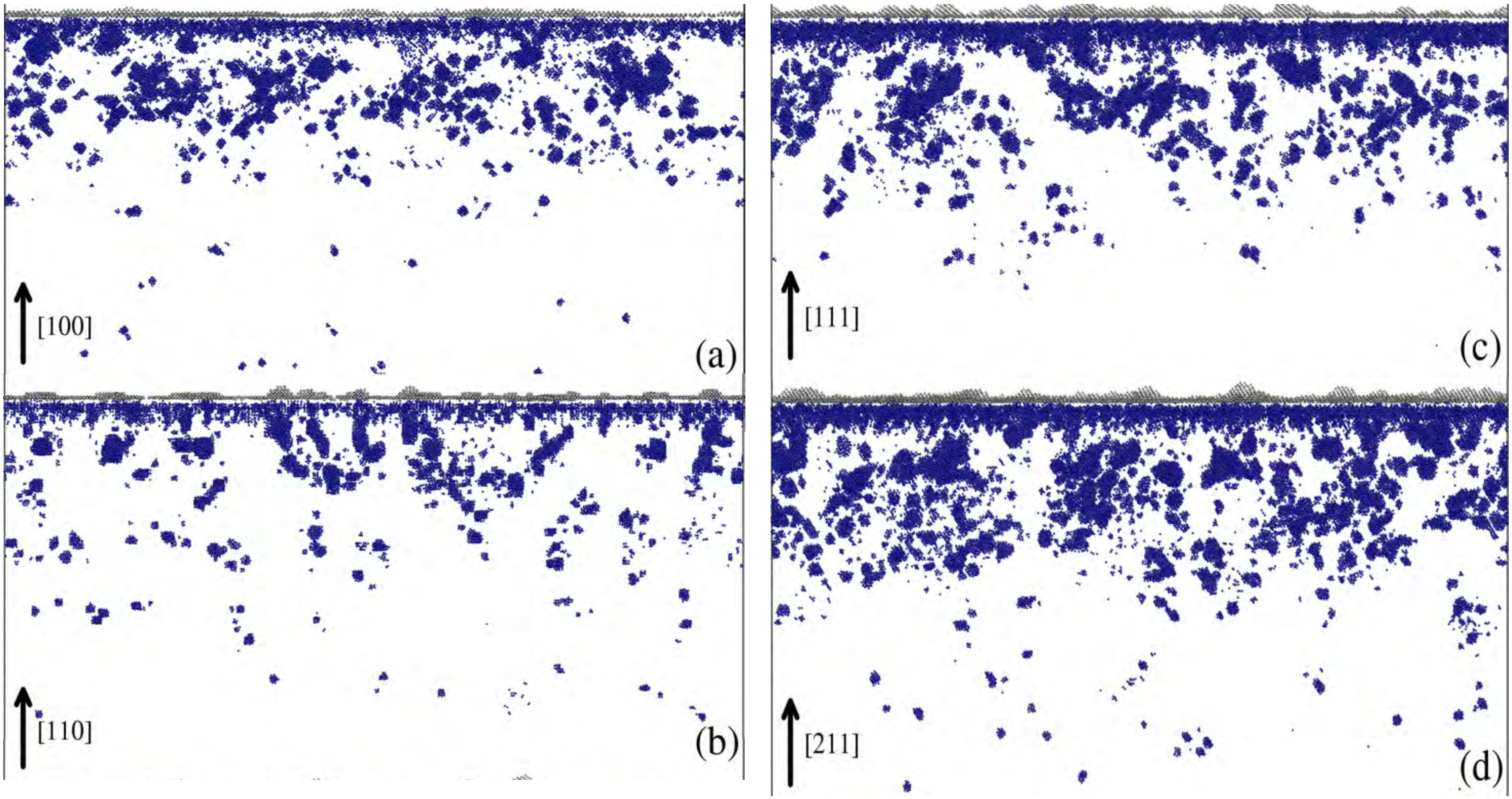

Helium distributions at a fluence of 3.3×10^{19} He-m^{-2}

Concentrated near-surface He layer also develops in (100) and (110) surfaces

*Hammond (UM), manuscript in preparation; *computations performed at* ***ALCF***

*Interactions of small mobile He clusters with surfaces**

- Small mobile He clusters, from aggregation of implanted helium in tungsten, migrate to the surface by Fickian diffusion and drift due to a thermodynamic driving force for surface segregation originating from the elastic interaction between the cluster and the surface.

$$\boxed{E_s(d) = -\frac{A_{s,n}}{d^3}}$$

$A_{s,n}$ increases with increasing cluster size n

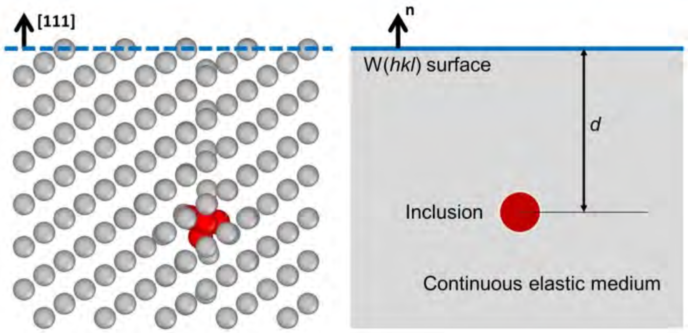

He_4 near W(211)

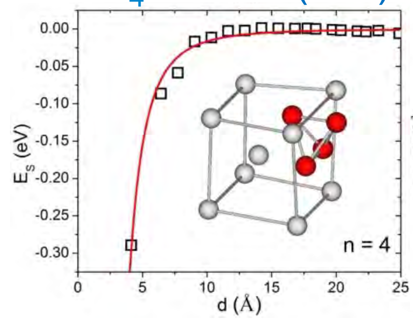

He_n near W(211)

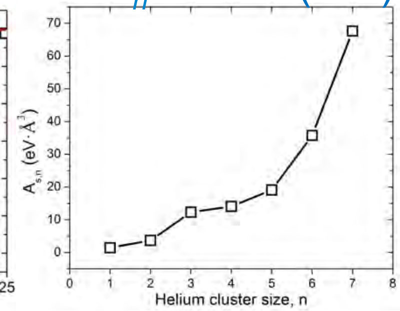

- As the clusters approach the surface, cluster reactions are activated with rates much higher than those in the bulk. The dominant ones are trap mutation (TM) reactions, generating immobile helium-vacancy complexes a few layers below the surface plane and tungsten surface adatoms: $W + He_n \rightarrow He_n\text{-}V_k + k\,W_{\underline{s}}$; $k \geq 1$

<u>Examples</u>:
He_4, He_5, and He_6 near W(110)

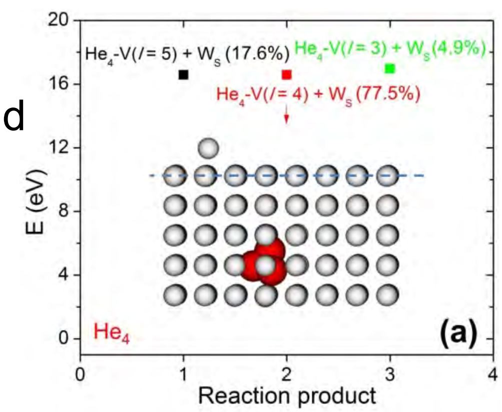

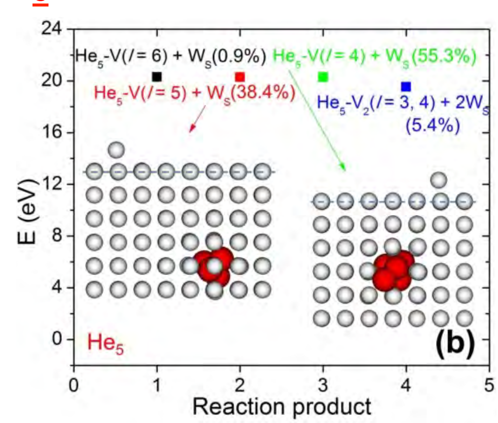

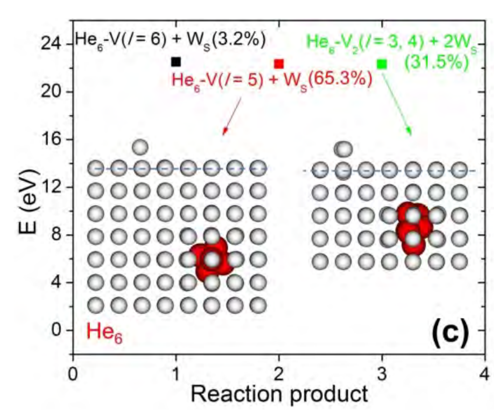

* Hu, Hammond, Wirth, and Maroudas, *J. Appl. Phys.* **115**, 173512 (2014);
Maroudas, Blondel, Hu, Hammond, and Wirth, *J. Phys.*: *Condens. Matter*, subm. (2015).

*Modified trap mutation near surfaces – orientation dependent**

Modified trap mutation (typically happens around He_7 in bulk) influences retention, He depth profile and bubble distributions

Sink	He_n (n = 1)	He_n (n = 2)	He_n (n = 3)	He_n (n = 4)	He_n (n = 5)	He_n (n = 6)	He_n (n = 7)
W(100)	D (100%)	D (19.1%) PD (5.9%) TM (75.0%) 1 W_V	D (1.1%) PD (11.6%) TM (87.3%) 1 W_V	D (2.1%) PD (74.6%) TM (23.3%) 2 W_V	D (4.1%) PD (85.3%) TM (10.6%) 2 W_V	D (2.3%) PD (36.9%) TM (60.8%) 3 W_V	D (3.1%) PD (27.4%) TM (69.5%) 4 W_V
W(110)	D (100%)	D (31.6%) PD (1.3%) TM (67.1%) 1 W_V	D (0.0%) PD (2.0%) TM (98.0%) 1 W_V	D (0.0%) PD (0.0%) TM (100%) 1 W_V	D (0.0%) PD (0.0%) TM (100%) 2 W_V	D (0.0%) PD (0.0%) TM (100%) 2 W_V	D (0.0%) PD (0.0%) TM (100%) 2 W_V
W(111)	D (35.4%) TM (64.6%) 1 W_V	D (1.2%) PD (0.0%) TM (98.8%) 1 W_V	D (1.6%) PD (0.0%) TM (98.4%) 1 W_V	D (0.0%) PD (0.0%) TM (100%) 2 W_V	D (0.0%) PD (0.0%) TM (100%) 2 W_V	D (0.0%) PD (0.0%) TM (100%) 3 W_V	D (0.0%) PD (0.0%) TM (100%) 3 W_V

D: He Desorption
PD: Partial Dissociation
TM: Trap Mutation
W_V: Tungsten Vacancy

For reactions of He_n clusters with n = 1, 2, and 3 see:

* Hu, Hammond, Wirth, and Maroudas, *Surf. Sci.* **626** (2014) L21-25.

*Xolotl-PSI**

- Xolotl (SHO-lottle) is the Aztec god of lightning and death
- Developed from 'scratch' for the SciDAC project, designed for HPC (current and emerging architectures – multicore, multicore+accelerator) to solve advection – reaction – diffusion cluster dynamics problems within spatially-resolved continuum domain (C++ with MPI and independent modules for physics, solvers and data management)
- 2D and 3D recently implemented
- Model considers continuum concentration of He, vacancies, interstitials and mixed clusters at spatial grid points, solving the coupled advection-reaction-diffusion equations

$$\delta_t \bar{C} = \phi \cdot \rho + D\nabla^2 \bar{C} - \nabla \bar{\nu} C - \bar{Q}(\bar{C})$$

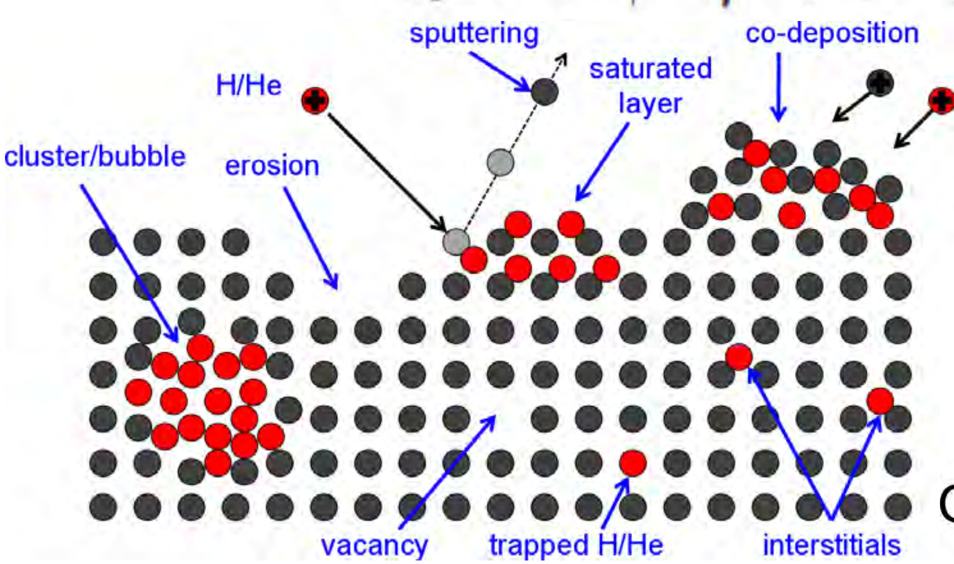

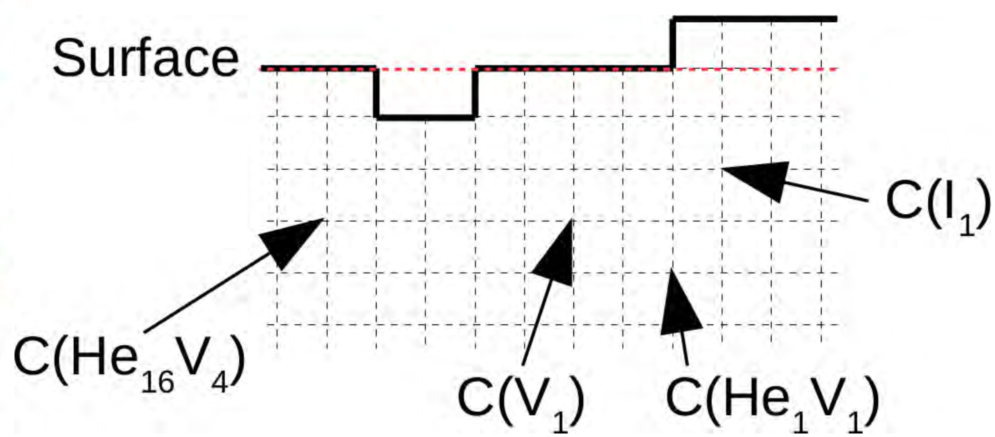

* Available at http://sourceforge.net/projects/xolotl-psi/

Initial results including advection (drift diffusion) & modified trap mutation

$$\frac{\partial C_i}{\partial t} = -\frac{3D_iA_i}{k_BT}\left(\frac{C_i(x)}{x^4} - \frac{C_i(x+h_x)}{(x+h_x)^4}\right)\frac{1}{h_x}$$

- Also include modification of He_x -> $He_xV_1 + I_1$ in which x depends on proximity to surface (parameterized based on MD simulation probability tables)

MD simulations Γ_{He} **~ 4E25 m^{-2}s^{-1}** **Xolotl simulations**

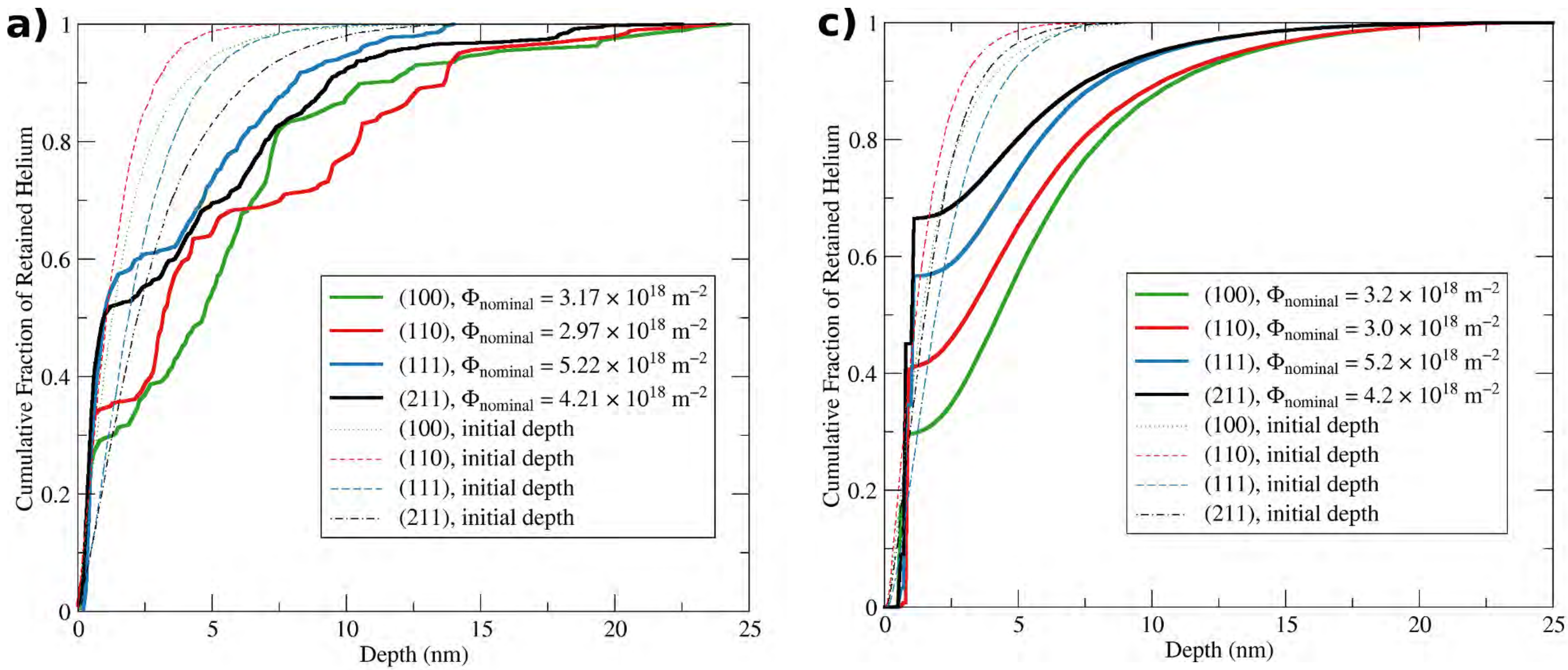

* Maroudas, Blondel, Hu, Hammond, and Wirth, *J. Phys. Cond. Matter.* **submitted**

Initial results including advection (drift diffusion) & modified trap mutation

Good early agreement does not persist at higher fluence: bubble bursting or modifications to the reaction rate constant are suspect. Future detailed comparisons of helium-vacancy cluster size distributions to help resolve this

MD simulations Γ_{He} **~ 4E25 m^{-2}s^{-1}** **Xolotl simulations**

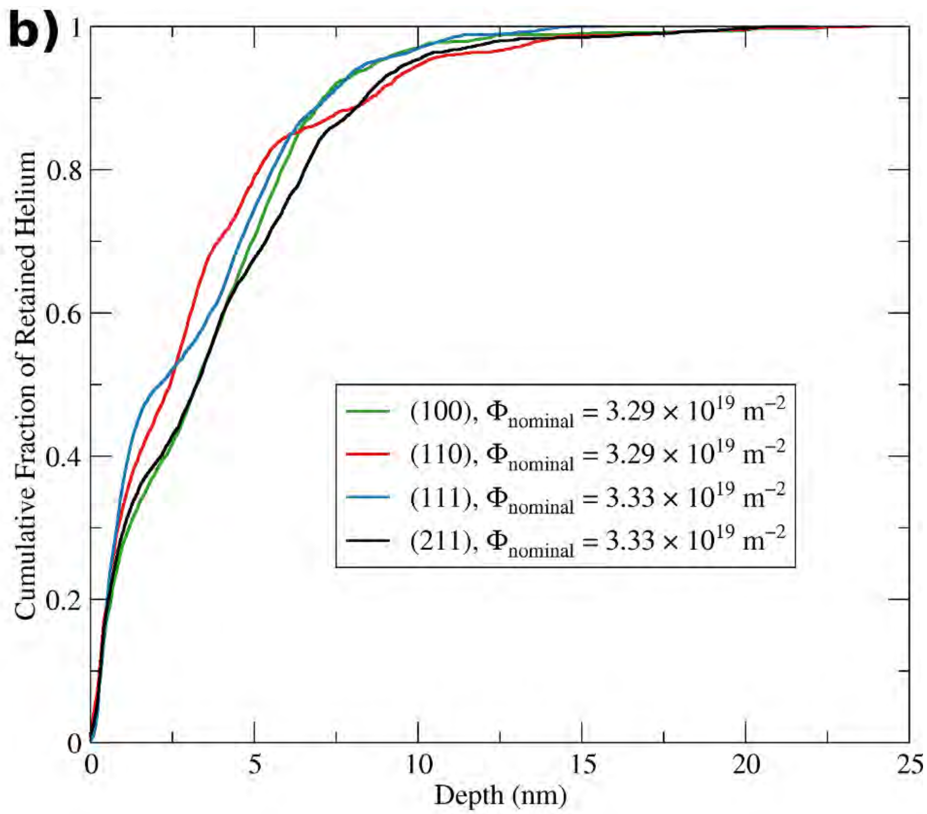

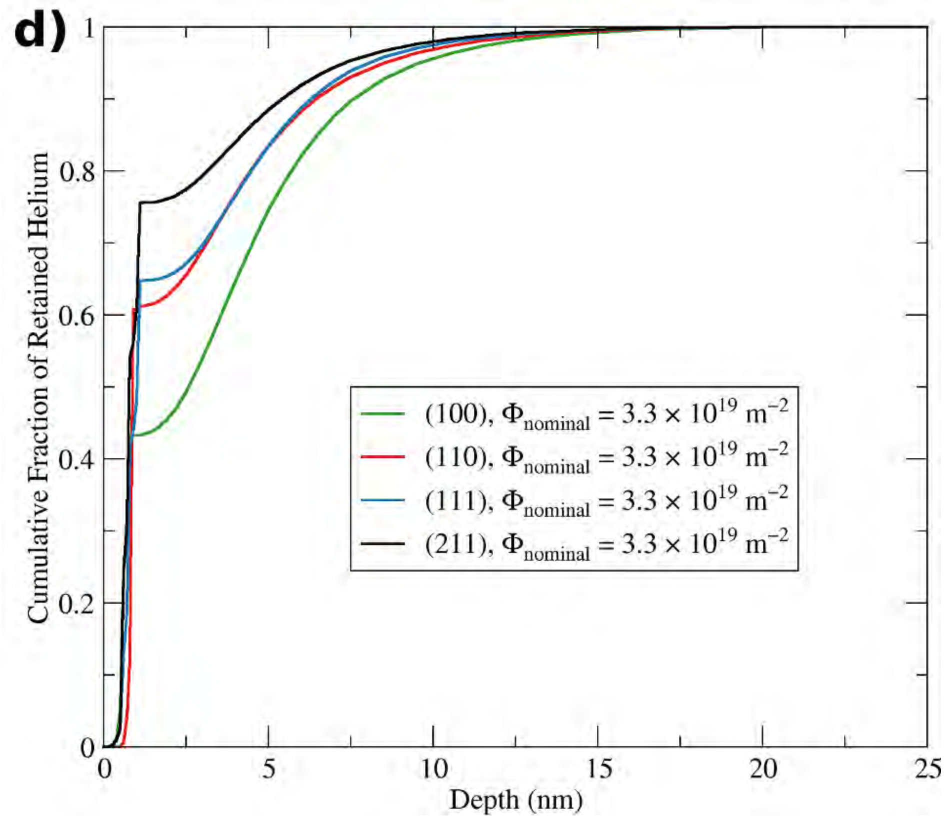

* Maroudas, Blondel, Hu, Hammond, and Wirth, *J. Phys. Cond. Matter.* **submitted**

More detailed Xolotl benchmarking to MD

100 eV He, 933 K

MD simulations **Γ_{He} ~ 4E25 m^{-2}s^{-1}** **Xolotl simulations**

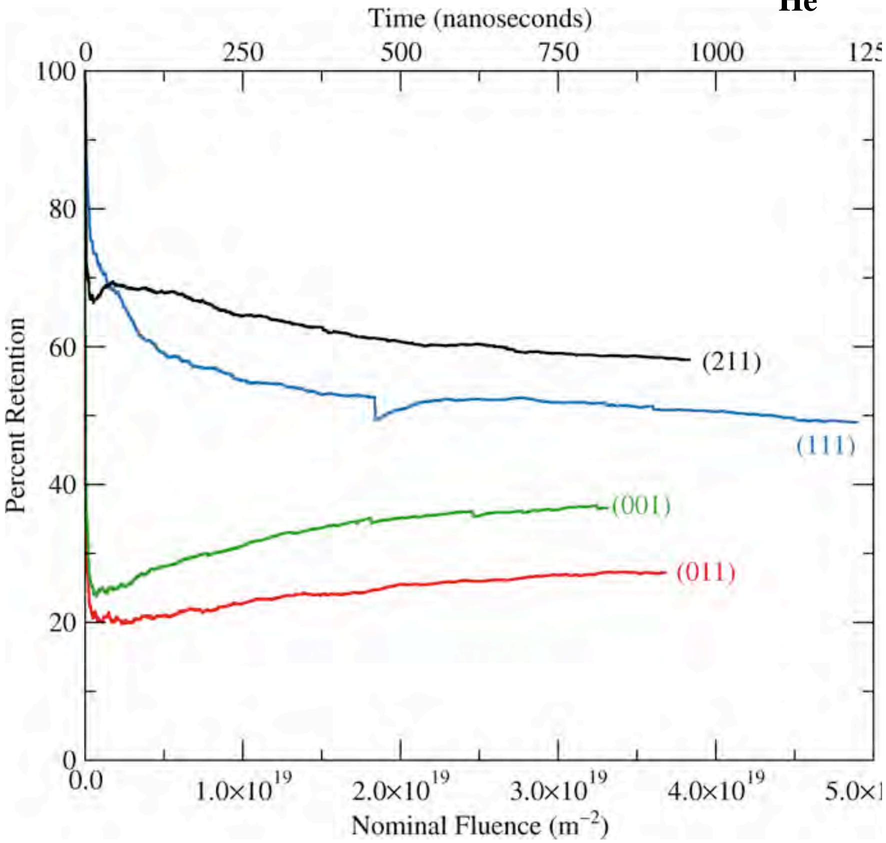

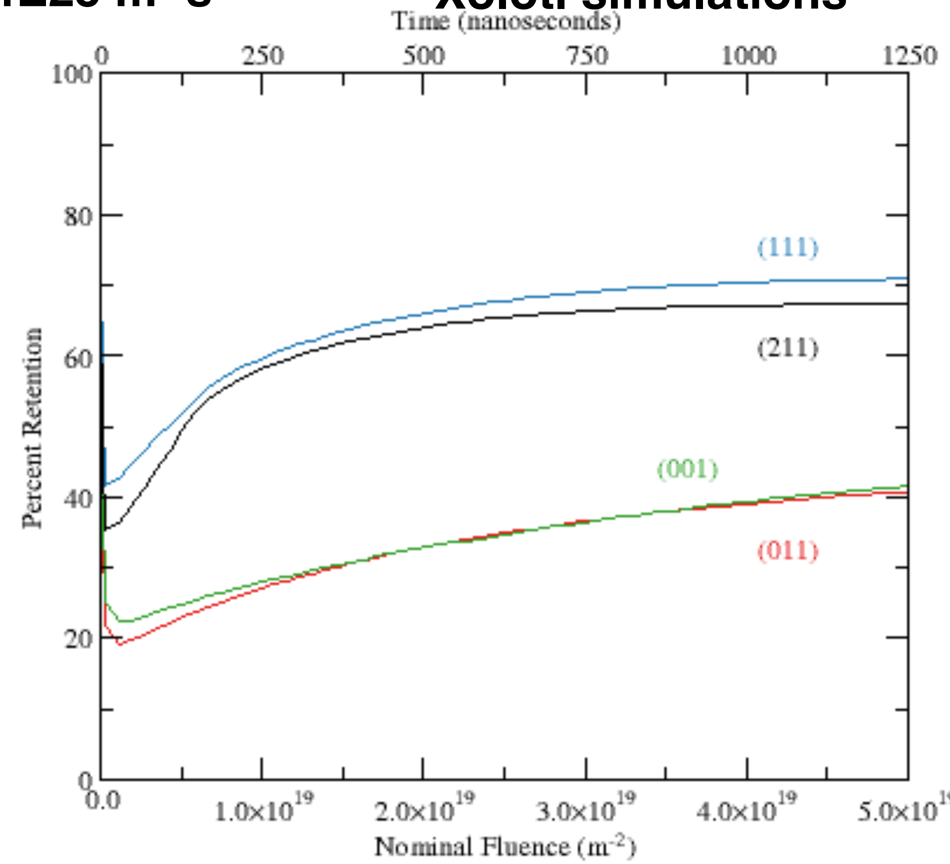

- Xolotl comparison/benchmarking to MD quite promising, but Xolotl is still missing (two) important physics:
  - Bubble bursting
  - Modified trap mutation below (211) implemented as (111)
  - Bubble coalescence

Visualization and analysis of large-scale atomistic simulations

Objective

• Identify damage to tungsten surface caused by helium bubbles

• Identify bubble shape evolution and possible coalescence

Impact

• Helium bubble detection and tracking

• Tungsten cavity detection and visualization

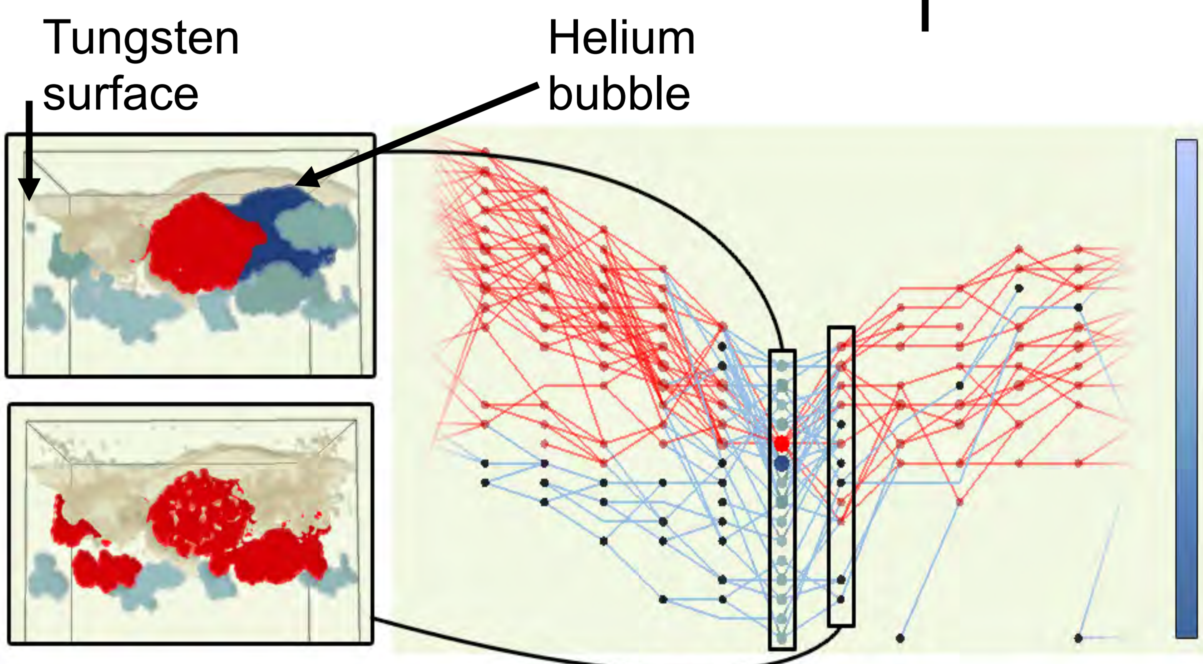

Accomplishments

• Integrated LAMMPS + VTK application for in-situ or post-process visualization pipeline.

* Widanagamaachchi, Hammond, Lo et al., *Eurographics Conference on Visualization* (2015)

Additional atomistic/Accelerated MD in progress

Deep bubble growth

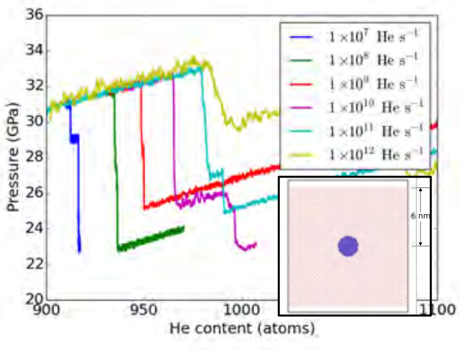

He bubble initially located in a spherical void of 277 vacancies. ~10^5 atoms at 1000 K.

As in the shallow bubble case, slower growth rates favor transitions with lower He content.

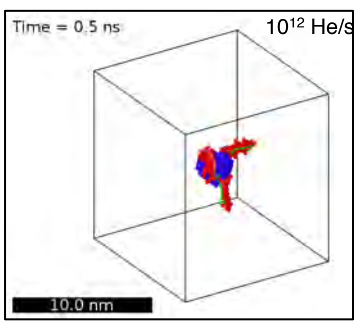

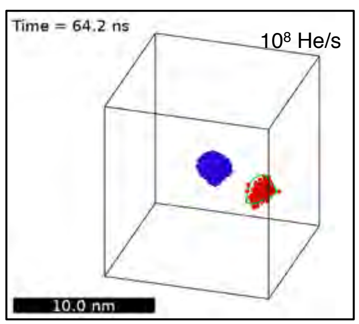

- At the over-driven rates simulated with MD, the tungsten matrix responds differently than at the slower rates representative of experiments.

Bubble growth near <111> screw dislocation

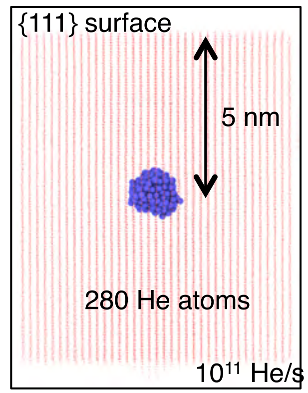

He bubble growth process strongly influenced by dislocations, which act as traps. For example, a He bubble nucleated in the at a screw dislocation (right) grows along the core and reaches the surface faster, as compared with the perfect crystal case (left).

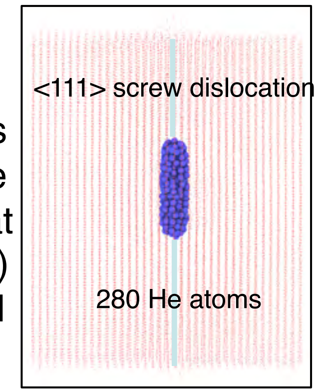

Bubble-bubble coalescence

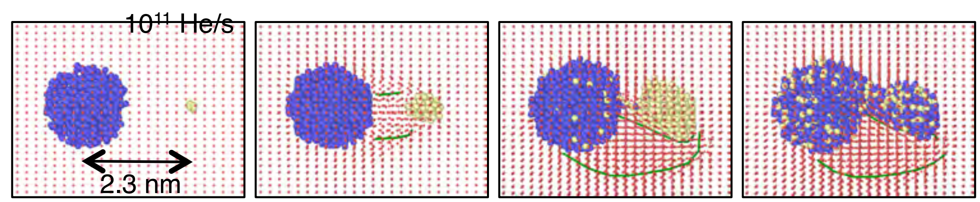

Simulations of bubbles growing in close proximity show a strong directionality of the growth process for the smaller bubble. The coalescence is characterized by the frequent nucleation and growth of connecting dislocations, eventually released from the bubbles as dislocation loops.

Sandoval, Uberuaga, Perez (LANL) unpublished results, in collaboration with BES funding (Voter)

Further Xolotl code development

•Verification of Xolotl 1D through cross code comparison against LAMMPS, Paraspace, and KSOME, as well as multiscale integration & benchmarking to large-scale MD

•Performance profiling performed against Paraspace by P. Roth (SUPER)

•Generalization of the system of equations in 2D and 3D, working closely with B. Smith and D. Wu (FASTMath).

•Significant improvement of the memory usage and performance run-time through strong interactions with B. Smith (FASTMath):

- 4th Order implicit Runge-Kutta ODE integrators with adaptive time steps allows much larger time steps while preserving accuracy
- Composite pre-conditions for linear systems with direct (1d) or multigrid (2 or 3d) solves for the diffusion terms with point-block Gauss-Siedel for reaction solves appears to be optimal and scalable solver for larger problems

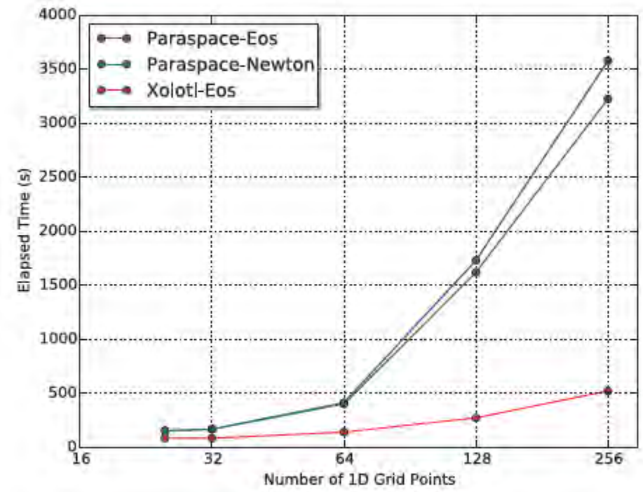

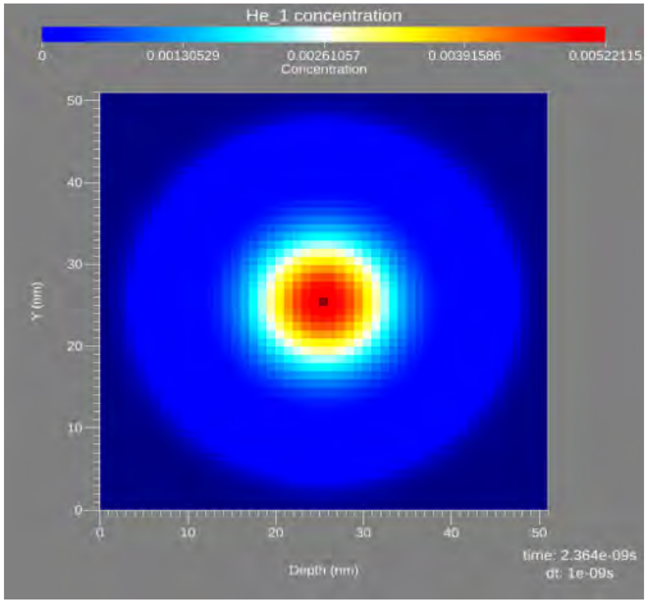

KMC simulation of He clustering below W surfaces

T=973K, Flux (Γ) of 100 eV He at 4E25 He $m^{-2}s^{-1}$

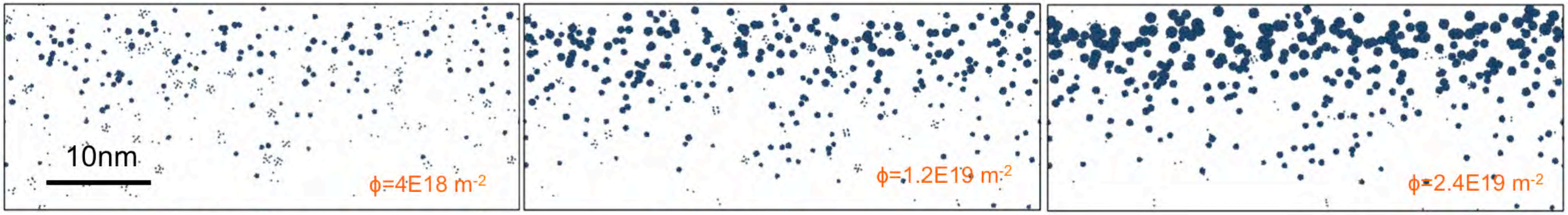

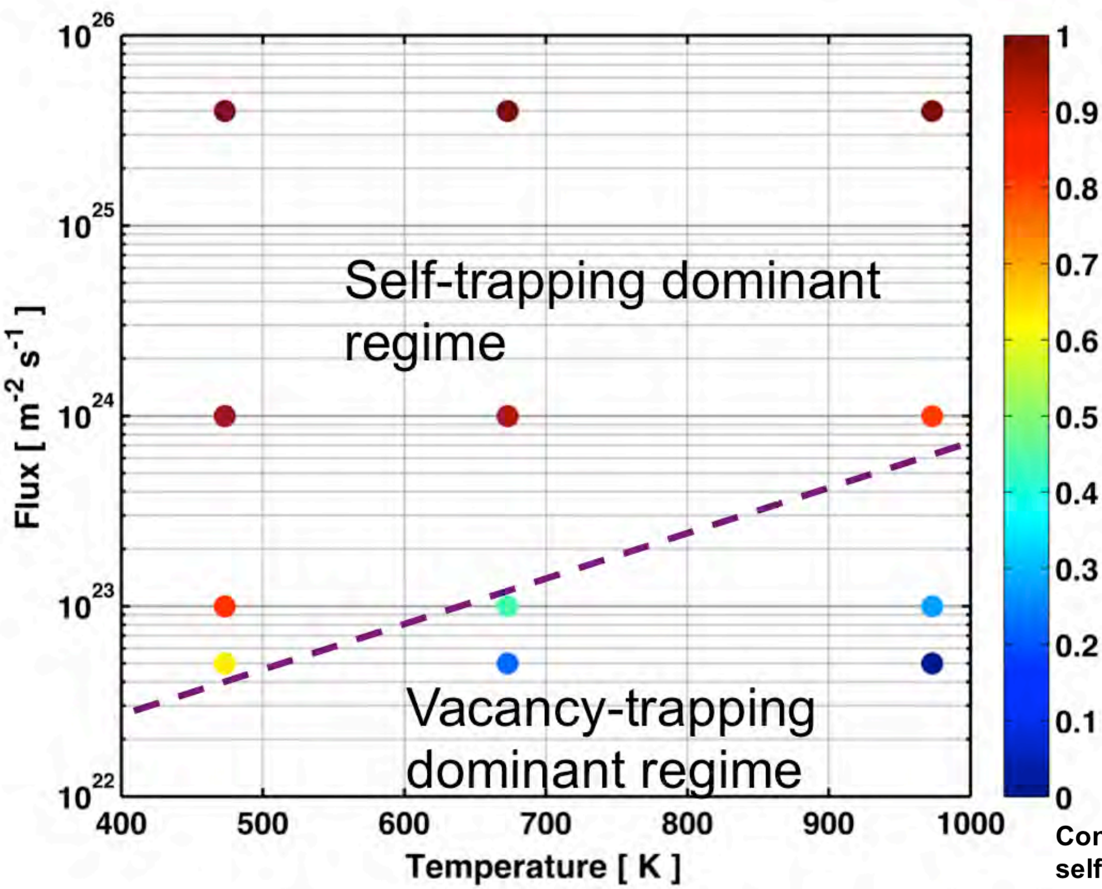

Kinetic Monte Carlo (KMC) simulations incorporating atomistic gas diffusion, clustering mechanisms used to extrapolate from ultra-fast MD implantation fluxes to experimentally relevant rates but limited to relatively short times O(seconds).

Indicate mechanism boundary of gas bubble nucleation mechanism f(Γ,T)

$$\text{Contribution of self-trapping} = \frac{\text{He retention rate with 0 appm vacancy}}{\text{He retention rate with 5 appm vacancy}}$$

He-H defect interactions in W

- Interatomic potential(s) derived to describe W-He* and W-He-H** interactions

Ab-initio data of H binding to He-H-V in W*

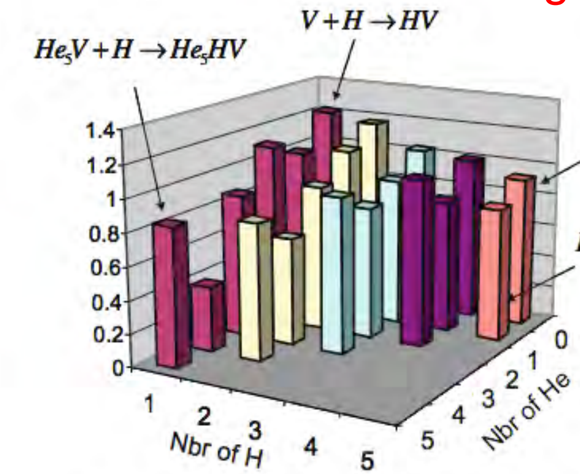

* Becquart & Domain, *JNM (1999)*

Atomistic result from potentials – Validating comparison

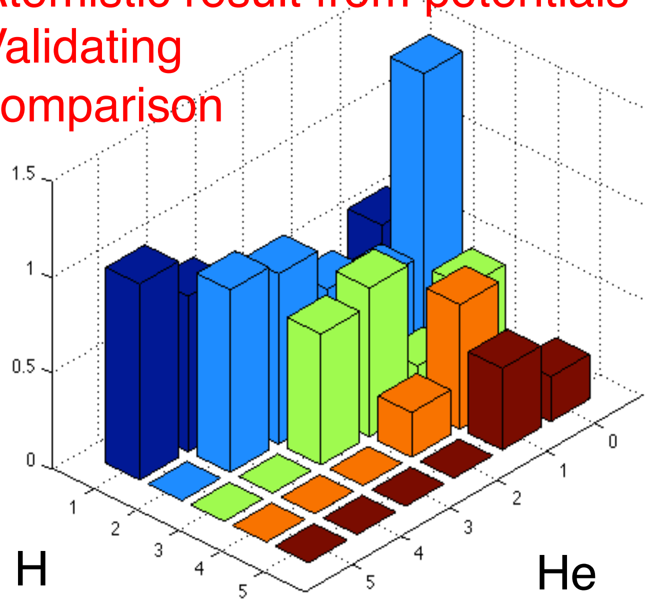

Validated potentials used to evaluate H partitioning to sub-surface He bubbles

- He is uniform, but H partitions to the bubble surface
- evaluating H storage capacity as function of bubble size & He pressure

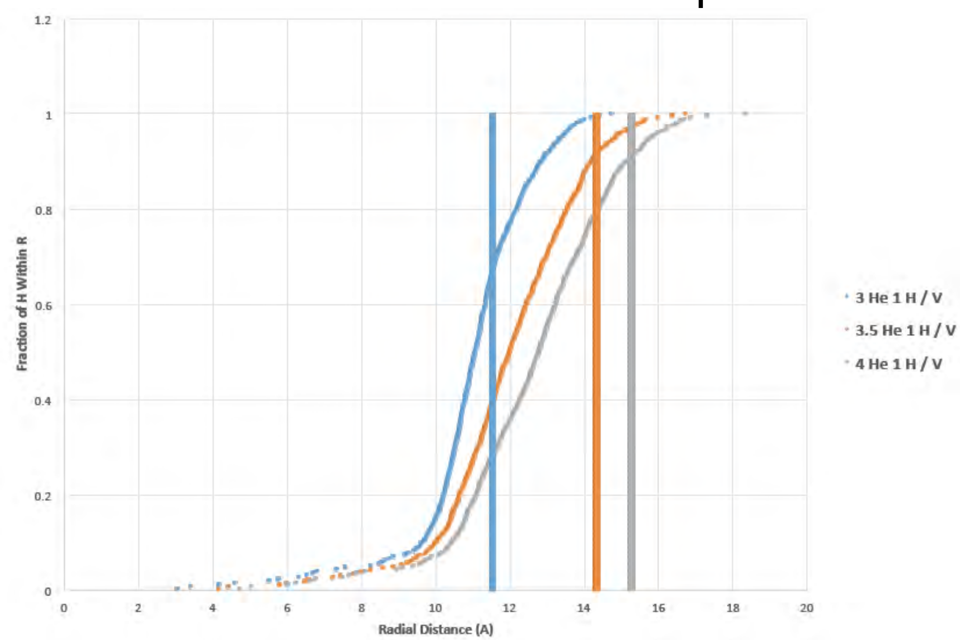

* Juslin and Wirth, *Journal of Nuclear Materials* **432** (2013) 61-66.
** Juslin and Wirth, *Journal of Nuclear Material* **438** (2013) 1221-1223.

Modeling Cascade Damage in Bulk Tungsten

- Spectrum of W PKAs due to 14-MeV neutrons shows a significant number of PKAs up to 280 keV of recoil energy or 196 keV of damage energy (E_{MD})
- Previously, primary defect damage database includes E_{MD} up to 100 keV
- New displacement damage data generated at 150 and 200 keV for 300, 1025, and 2050 K
- Data at 150 and 200 keV follow the trend of defect production curve (N_F) for $E_{MD} > 30$ keV
- KMC simulations of irradiation damage accumulation due to 14 MeV neutrons are currently underway

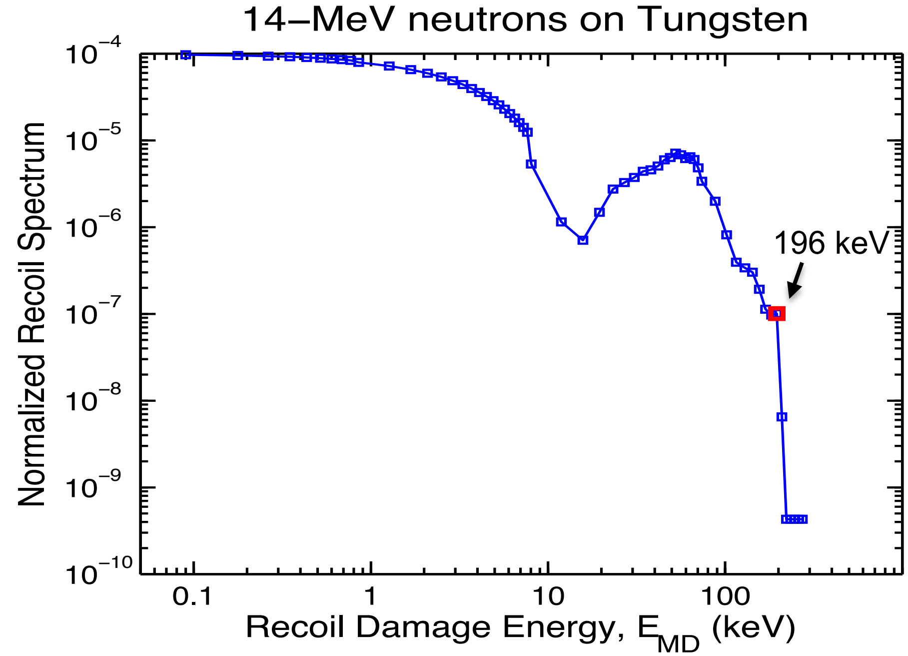

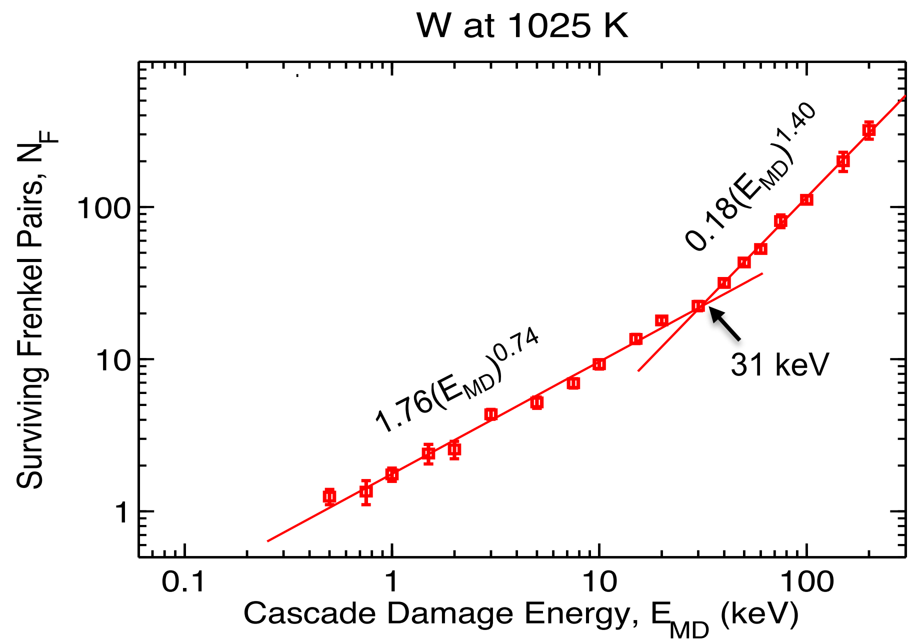

* Setyawan, Selby, Juslin, Stoller, Wirth and Kurtz, *J. Phys. Cond. Matter* **27** (2015) 225402.

Dose Dependence of Vacancy Cluster Densities and Sizes

- With increasing dose rate:
  - Number density of vacancies increases
  - Vacancy cluster density decreases
  - Average vacancy cluster size decreases
- Fraction of visible clusters:
  - 10^{-8} dpa/s - saturates at 95% of the vacancy population
  - 10^{-4} dpa/s –reaches 55% of the vacancy population at 1 dpa
  - Visible clusters - 2 nm diameter or about 300 vacancies
- Vacancy cluster sizes at 10^{-8} dpa/s:
  - Grow larger than at higher dose rates due to the greater time between cascade insertions permiting more defect diffusion
  - Di-vacancies are not stable, which suppresses nucleation of new clusters
- No formation of SIA clusters
  - SIAs quickly diffuse to grain boundaries
  - SIAs are more likely to recombine with the increasing population of vacancy clusters

Dose rate has significant effect on void growth

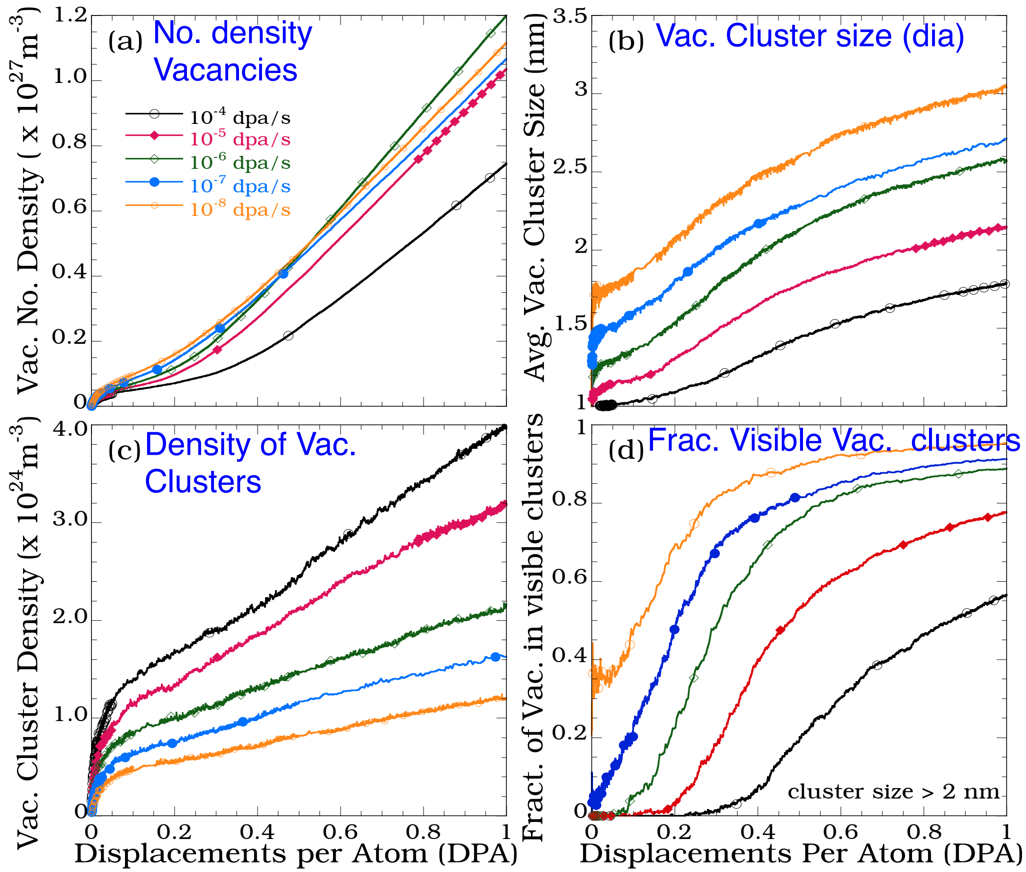

Summary & Future Efforts

• Effort in boundary physics modeling to track impurities, evaluate sheath effects and improve the coupling across the plasma – surface interface

• Multiscale materials simulations being used to evaluate He bubble nucleation, gas bubble evolution and impact on tungsten surfaces
- Results clearly indicate highly mobile He self-traps and small mobile He clusters undergo trap mutation ($He_x \rightarrow He_xV_y + I_y$) that immobilizes clusters leading to nucleation of growing, highly over-pressurized He bubbles. Bubble growth through trap mutation & loop-punching produce substantial surface roughness. Growing bubbles eventually rupture
- Promising results for benchmarking of Xolotl against MD (& KMC, though not shown)
- Strong influence of implantation flux on bubble size distributions as a function of depth – impact of (radiation/thermal) damage still to be resolved

• Initial framework for performing uncertainty analysis of the impact of uncertainty in He-vacancy thermo-kinetics on He bubble nucleation, retention and W surface response & directly validating the multiscale models against experimental data

• Future effort to understand He-H synergies & impact of He gas bubble formation on H/D/T recycling and retention

W-He interaction potentials

- **Interatomic potentials**
  - **W-W: Ackland FS pot., with Juslin short range***
    - Reasonable, N-body/EAM style potential among 20+ other published potentials
  - **Juslin W-He pair pot***
    - Wilson 1972, Henriksson 2004 potentials single interstitials not in agreement with DFT
  - **Beck He-He pair pot. (with Morishita short range fit)****
    - Aziz, Janzen potentials similar

W potential modified by Juslin for High-energy collisions

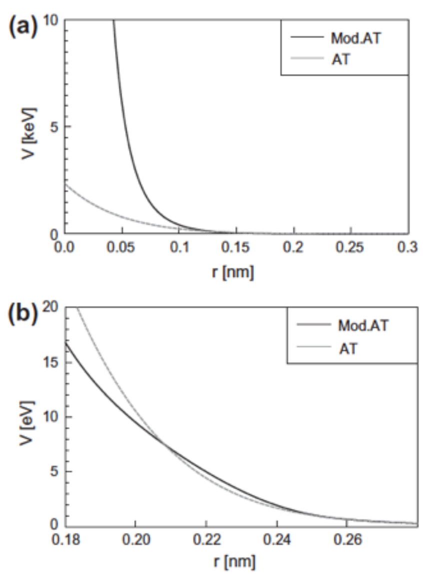

Fig. 2. The modified pair potential part of the Ackland–Thetford tungsten potential compared to the original. (a) Shows how much softer the original AT is compared to the ZBL at less than about 1.4 Å, while (b) shows a closer view of the distances relevant to interstitial properties.

W vacancy cluster binding energies 'track' DFT results but with an offset

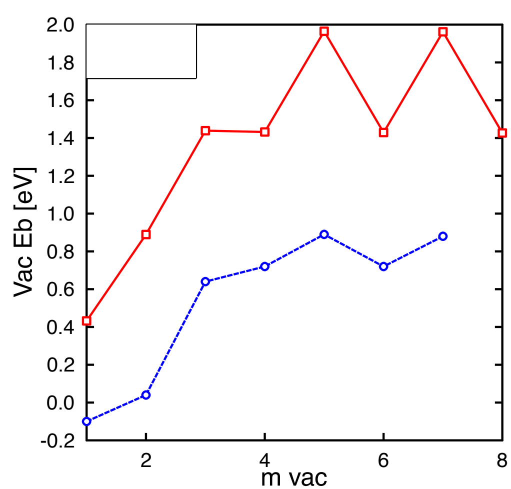

W-He potential – functional form (repulsive pair), agrees with DFT data

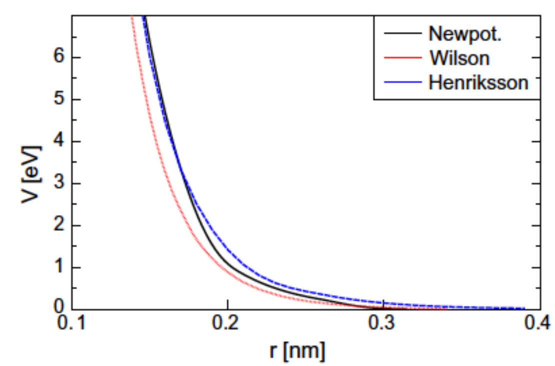

Fig. 1. The new W–He pair potential compared to the potentials by Wilson and Henriksson.

* Juslin and Wirth, *J. Nuc. Mat.* **432** (2013) 61.
** Morishita et al., *NIMB* **202** (2003) 76.